Tellus (1988), *40B*, 270–284

A comparison of models for deriving dry deposition fluxes of O_3 and SO_2 to a forest canopy

By TILDEN P. MEYERS and DENNIS D. BALDOCCHI, *National Oceanic and Atmospheric Administration, Air Resources Laboratory, Atmospheric Turbulence and Diffusion Division, P.O. Box 2456, Oak Ridge, Tennessee 37831, USA*

(Manuscript received 9 September 1987; in final form 21 January 1988)

ABSTRACT

4 canopy models, representing the various classes of models that are currently used to estimate gaseous deposition to plant canopies are presented. The predictive capabilities of the models are evaluated with direct eddy correlation measurements of SO_2 and O_3 fluxes to a deciduous forest for both well-watered and water-stressed conditions. By increasing the degree of detail of the exchange-governing physical processes from the more simple single layer model to the more detailed multi-layer models, the predictions of the deposition rates improved by 40–50% as determined from the root mean square error (rmse). We also found by including the effect of water stress in the stomatal resistance formulations, the rmse of the predictions were decreased by generally 50% for the models that were examined.

1. Introduction

Direct measurements of dry deposition fluxes are difficult to make on a routine basis. Consequently, the use of models has been advocated as a means of deriving estimates of dry deposition fluxes routinely (Hicks et al., 1987). Scientists at the NOAA/ARL Atmospheric Turbulence and Diffusion Division have developed a hierarchy of dry deposition models. These deposition models range in complexity from the simple multiple resistance models (Hicks et al., 1987; Baldocchi et al., 1987) to the more detailed canopy turbulence models (Baldocchi, 1988; Meyers, 1987). The complexity of these models differ in two major aspects. The simpler models treat the plant canopy as a "big leaf" surface which is partitioned into shaded and sunlit portions to account for differences in stomatal resistances. The "big leaf" models are relatively easy to implement because they require measurements of environmental, physiological, and structural variables that are easily obtained. The more detailed models separate the canopy into multiple layers and treat the physics of the transfer processes more rigorously. They also incorporate canopy radiative transfer models to obtain a more realistic distribution of the net (R_n) and photosynthetically active radiation (PAR) throughout the canopy in order to compute dependent nonlinear biological processes such as stomatal conductance and transpiration more accurately. These models require more detailed information on canopy structure and the state of atmospheric turbulence.

In this paper, we evaluate several types of models by comparing the predicted fluxes of SO_2 and O_3 with direct measurements for both water-stressed and well-watered conditions. Testing models over a wide range of water deficit conditions is crucial because the surface uptake resistance (mainly stomatal) is the limiting factor governing SO_2 and O_3 deposition and it is strongly influenced by soil moisture content. The models that are examined and tested include a multiple resistance model (Hicks et al., 1987), a hybrid "big-leaf"/multi-layer model (Baldocchi et al., 1987), a multi-layer "K-theory" model (Baldocchi, 1988), and a higher-order closure model (Meyers, 1987; Meyers and Paw U, 1987).

These four models represent the classes of current models that are presently used to derive estimates of dry deposition rates of SO_2 and O_3 from measured meteorological and concentration data.

2. Single layer (big leaf) models

2.1. "Big leaf" multiple resistance model

The "big leaf" model (hereafter known as model I) is based on a one-dimensional framework and is applicable over extended, homogeneous canopies in relatively uniform terrain. This model (as with the other models presented) assumes that the interior of the leaf is a perfect sink (i.e., the concentration of the chemical species of interest in the leaf interior is zero) and that the soil is not a source for SO_2 and O_3. Hence, this model is only applicable for circumstances where it is known that the transfer of the pollutant is always directed towards the surface.

The downward chemical flux is estimated as the product of the deposition velocity V_d and the concentration of the chemical species of interest. The deposition velocity is an integral of the physical, chemical and biological processes that govern the rate of exchange between the atmosphere and the receptor surface. It characterizes deposition to a forest canopy using a resistance analog for transfer shown in Fig. 1. The primary resistances to pollutant uptake are identified as the aerodynamic resistance (R_a), the quasi-laminar boundary layer resistance (R_b), and the surface uptake or canopy resistance (R_c), such that

$$V_d = (R_a + R_b + R_c)^{-1} \tag{1}$$

Note: an upper case "R" refers to the resistance on a land area basis, while "r" is used for resistances on a leaf area basis.

The ability of the atmosphere to vertically transfer trace gas constituents by turbulent diffusion is characterized by R_a, which is governed by both mechanical mixing and buoyancy. The standard deviation of the wind direction (σ_θ) contains information on stability and can be combined with measurements of the mean wind speed ($\bar{u}$) (see Hicks et al., 1987) to provide estimates of R_a.

$$R_a \simeq 4(\bar{u}\sigma_\theta^2)^{-1}, \quad \text{neutral to stable conditions,} \tag{2a}$$

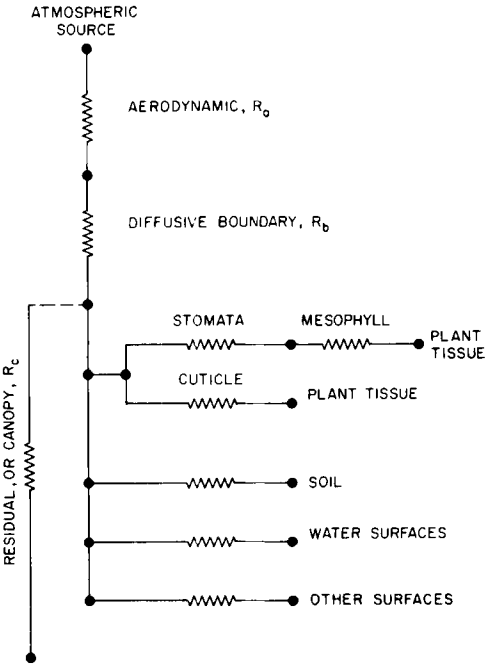

Fig. 1. Resistance network for transfer from atmosphere through diffusive boundary layer into surface receptors.

$$R_a \simeq 9(\bar{u}\sigma_\theta^2)^{-1}, \quad \text{unstable conditions.} \tag{2b}$$

The quasi-laminar boundary layer resistance (R_b) is an "excess" resistance, associated with diffusive transfer through the quasi-laminar boundary layer in contact with the receptor surfaces. Based on experimental and theoretical considerations (Wesely and Hicks, 1977; Hosker, 1986, R_b is generally computed as:

$$R_b = (2/ku_*)\cdot(D_t/D_c)^{2/3} \tag{3}$$

where k is von Karman's constant (0.4), u_* is the friction velocity, D_t is the thermal diffusivity of air and D_c is the molecular diffusivity of the gas of interest. After determining R_a, a consistent value of u_* is obtained from the near-neutral approximation $R_a \cong \bar{u}/u_*^2$.

The surface uptake or canopy resistance (R_c) is a composite resistance, comprised of the transfer through the leaf stomata (r_s) and into the mesophyll tissue (r_m), and to transfer directly into the leaf cuticular membrane (r_{cut}), the soil (r_{soil}), and any other surface component that may be a

sink. The stomatal resistance is a function of photosynthetically active radiation (PAR), leaf temperature (θ_ℓ), leaf-air vapor pressure deficit (vpd), internal CO_2 concentration, leaf water potential (ω), and leaf age and position (see Jarvis, 1976; Mansfield, 1985). The stomatal resistance generally responds non-linearly to its controlling factors and is usually calculated with a multiplicative model:

$$r_s = r_{s,\min}(1 + \beta/I)/f(\theta_\ell)\cdot f(\omega)\cdot f(\text{vpd}) \quad (4)$$

where $r_{s,\min}$ is a species-dependent minimum stomatal resistance and β is a response coefficient equal to the incident PAR (I) on the leaf surface at twice $r_{s,\min}$. The factors $f(\omega)$, $f(\text{vpd})$ and $f(\theta_\ell)$ represent correction factors for leaf water potential, leaf-air vapor pressure deficit, and leaf temperature, respectively, and range between 0 and 1 (see Jarvis, 1976).

The computation of canopy stomatal resistance in the "big leaf" model depends on the fractions of sunlit and shaded leaf area and the flux density of PAR on those leaves. By assuming the foliage has a spherical leaf angle distribution, the sunlit (L_s) and shaded (L_{sh}) leaf area can be estimated as (Monteith, 1973).

$$L_s = [1 - \exp(-K\cdot\text{LAI})]/K \quad (5a)$$

$$L_{sh} = \text{LAI} - L_s \quad (5b)$$

where K is the extinction coefficient ($K = 0.5/\cos\alpha$, α is the zenith angle) and LAI is the leaf area index. Incorporating the mesophyll resistance (r_m), the non-cuticular canopy resistance as a function of PAR is computed as:

$$R_s = 1/[L_s/(r_s(I_s) + r_m) + L_{sh}/(r_s(I_{sh}) + r_m)], \quad (6)$$

where I_s and I_{sh} are the flux densities of PAR on the sunlit and shaded leaves, respectively. I_s is computed as $I_s = 0.5I_b/\cos\alpha + 0.5I_{sh}$. The beam ($I_b$) and diffuse ($I_{sh}$) PAR incident on the canopy are approximated with the method of Weiss and Norman (1985). The only required inputs are latitude, longitude, time of day, day of the year, and incoming global radiation. The beam component is multiplied by 0.5, which is the cosine of the mean leaf angle ($\pi/3$) in the direction of the sun and is divided by $\cos\alpha$ to obtain the mean flux density (I_b) incident on the sunlit leaves (Ross, 1976). The average diffuse PAR for all shaded leaves is assumed to be one-half the incoming value above the canopy, based on the measurements and computations of Baldocchi et al. (1985).

The foliage uptake resistance per unit ground area (R_f) is obtained by combining the weighted parallel stomatal resistance of the sunlit and shaded leaf area and the foliar cuticular resistance.

$$1/R_f = [1/(R_s) + \text{LAI}/r_{cut}]. \quad (7)$$

The bulk canopy or surface uptake resistance (R_c) can then be determined by correctly summing the parallel resistances to the foliage, soil and any other receptor surface type.

Measurements needed to drive the model include the mean wind speed ($\bar{u}$), standard deviation of the wind direction (σ_θ), global radiation (R_g), air temperature ($\bar{\theta}$), and concentration of the pollutant above the canopy. Knowledge of the leaf area index is the only plant structural information required. The stomatal resistance parameters $r_{s,\min}$ and β are plant species dependent. These values are generally obtained from the literature in the absence of measurements.

2.2. *Hybrid "big leaf"/multi-layer model*

The hybrid "big-leaf"/multi-layer model (see Baldocchi et al., 1987) (hereafter known as model II) is similar to model I except that a more detailed representation of the aerodynamic (R_a) and canopy resistance (R_c) is included. The canopy aerodynamic resistance is computed as being proportional to the amount of momentum transferred to the canopy (see Wesely and Hicks, 1977; Hosker, 1986). The relationship between canopy stomatal conductance and PAR is computed via coupling the multi-layer canopy radiative transfer model of Norman (1979) with eq. (4) to provide profile estimates of stomatal resistance on the sunlit and shaded leaves throughout the canopy. Measurements needed to perform model calculations are the same as with model I, but include measurements of u_* and atmospheric stability, in terms of the Monin-Obukhov length scale.

3. Multi-layer models

The multi-layer models build upon the hybrid "big-leaf"/multi-layer model by including more

detail about the turbulent transfer processes within the canopy and molecular diffusion through viscous sublayers at the leaf scale. In addition, multi-layer models can accommodate bi-directional fluxes within the canopy as a result of soil surface emissions of some chemical species (e.g., ammonia, nitrogen dioxide).

The time- and volume-averaged conservation equation for a gas pollutant of concentration c, for horizontally homogeneous conditions, is

$$\frac{\partial\langle\bar{c}\rangle}{\partial t} = 0 = \frac{-\partial\langle\overline{w'c'}\rangle}{\partial z} + \text{source/sink}, \tag{8a}$$

$$\text{where source/sink} = \frac{D_c}{V}\int\int_S \frac{\partial\bar{c}}{\partial n}\,ds, \tag{8b}$$

where brackets denote a volume average (Finnigan, 1985; Raupach et al., 1986), the overbar indicates a temporal average, primes (′) are departures from the temporal mean, w is the vertical wind component, and n is a unit vector directed away from and normal to the differential plant element area (S), within the averaging volume (V). For steady state conditions the divergence of the vertical turbulent flux is balanced by the sink term which can be expressed as

$$\text{sink} = -A(z)\,\bar{c}(z) \times\left[\frac{1}{(r_b(z)+r_s(z)+r_m)} + \frac{2}{(r_b(z)+r_{cut})}\right] \tag{9}$$

where $\bar{c}(z)$ is the mean concentration of the pollutant of interest, A is the plant area density, $r_b(z)$ is the leaf boundary layer resistance and $r_s(z)$, and r_{cut} are the stomatal and cuticular resistances, respectively. The leaf boundary layer resistance (r_b) is the resistance to molecular diffusion across the quasi-laminar leaf boundary layer, and is evaluated as

$$r_b = \ell/(D_c \cdot \text{Sh}) \tag{10}$$

where ℓ is a characteristic leaf length and Sh is the Sherwood number. Relationships for Sh are derived from heat transfer over flat plates (Eckert and Gross, 1963; Grace and Wilson, 1976). A canopy radiative transfer model (Norman, 1979) was used to provide estimates of PAR for the sunlit and shaded leaves for each layer in the model domain. The leaf and soil radiative properties that were used in the model are taken from Baldocchi et al. (1985), and are listed in Table 1 along with the values for $r_{s,min}$, r_m, r_{cut}. The numerical value of the stomatal resistance listed in Table 1 is for water vapor diffusion and must be corrected by the appropriate molecular diffusivity for the pollutant gas of interest assuming similarity in the diffusion pathways.

Near the soil surface, the flux divergence of the pollutant of interest is assumed to be zero and the flux is equal to the soil uptake (or emission) rate. The rate of exchange of a pollutant gas at the soil is computed based on the experimental work of Schuepp (1977).

Table 1. *Parameters used to make model computations*

Variable	Value	Units	
LAI	5	—	Hutchison et al. (1986)
canopy height (H_c)	23	m	Hutchison et al. (1986)
$r_{s,min}$	100	s m^{-1}	measured
β	40	W m^{-2}	measured
leaf length l	0.10	m	measured
bulk canopy drag coefficient	0.016	—	Verma et al. (1986)
wind extinction coefficient	6.95	—	measured
optimal leaf temperature (T_0)	27.5	°C	
maximal leaf temperature (T_{max})	45	°C	
minimal leaf temperature (T_{min})	10	°C	
r_m	0	s m^{-1}	
$r_{cut}(O_3)$/LAI	3000	s m^{-1}	
$r_{cut}(SO_2)$/LAI	1500	s m^{-1}	
$r_{soil}(O_3$ & $SO_2)$	100	s m^{-1}	
leaf reflectivity PAR	0.11	—	Baldocchi et al. (1985)
leaf transmissivity PAR	0.16	—	Baldocchi et al. (1985)
soil reflectivity PAR	0.033	—	Baldocchi et al. (1985)
leaf reflectivity NIR	0.43	—	Baldocchi et al. (1985)
leaf transmissivity NIR	0.26	—	Baldocchi et al. (1985)

The explicit use and reference to these variables are presented in the papers describing models I through IV.

3.1. K-theory model

In this model (hereafter known as model III), first-order-closure assumptions are made to close the set of equations (see Baldocchi (1988)). This is achieved by implementing the concepts originally proposed by Waggoner (1975), Shreffler (1976; 1978) and Murphy et al. (1977) for pollutant exchanges within plant canopies. With this approach, vertical turbulent flux of a pollutant gas inside a canopy is computed as the product of an eddy exchange coefficient (K_c) and the local concentration gradient:

$$\overline{w'c'}(z) = -K_c(z)\frac{\partial}{\partial z}\bar{c}(z), \tag{11}$$

where K_c is determined from momentum balance theory (see Thom, 1975).

Eqs. (8) and (11) were solved numerically on 40 equidistant grid points within the canopy.

The input variables needed to run the model include measurements of mean wind ($\bar{u}$), friction velocity (u_*), Monin-Obukhov scale length (L), air temperature, and global radiation. Structural information includes the vertical distribution of leaf area, an effective leaf drag coefficient (C_d), canopy height, and leaf size.

3.2. Higher-order-closure model

The higher-order-closure model (model IV) is a steady-state, one-dimensional, volume-averaged model. It uses the conservation equations for momentum and mass transfer to model the canopy flow field and pollutant transfer (see Meyers and Paw U (1986, 1987), Meyers (1987). In this case, the use of explicitly calculated resistances is abandoned, except in the calculation of the source/sink strength for heat, water vapor, and any other gaseous constituent for each layer within the canopy. The model by Norman (1979), which was incorporated into models II and III, was also used in model IV to describe the radiation field and was coupled with leaf energy balance equations to provide estimates of net radiation, heat and water vapor flux, leaf vapor pressure deficits and leaf temperature for nine leaf angle classes of sunlit and shaded leaves throughout the canopy (see Meyers and Paw U (1987), as needed for the computation of stomatal resistance. In higher-order closure models, rate equations are carried for the second and (sometimes) third moments, thereby abandoning the need to relate vertical turbulent fluxes directly to local concentration gradients. It is believed that the modeled results are less sensitive to closure of the equations at a higher order. The time- and volume-averaged conservation equation for the vertical turbulent flux of a pollutant with concentration c is given by

$$\frac{\partial\langle\overline{w'c'}\rangle}{\partial t} = 0 = \underbrace{-\langle\overline{w'^2}\rangle\frac{\partial\langle\bar{c}\rangle}{\partial z}}_{G} \underbrace{-\frac{\partial\langle\overline{w'w'c'}\rangle}{\partial z}}_{T}$$

$$\underbrace{-\left\langle\overline{c'\frac{\partial p'}{\partial z}}\right\rangle}_{P} + \underbrace{g\beta\langle\overline{\theta'c'}\rangle}_{B} \tag{12}$$

where G is a gradient production term, T is a transport term, and P is a pressure term (sink) that acts to decorrelate w and c. The gravitational constant g, potential temperature θ and thermal expansion coefficient $\beta = \theta^{-1}$ comprise the buoyancy term B which can be either a source (unstable conditions) or sink (stable conditions) to the $\langle\overline{w'c'}\rangle$ budget. In eq. (12) and remaining equations, dispersive terms or fluxes which arise from correlations between deviations from spatial averages (see Finnigan 1985) are thought to be small and have been neglected. Additional equations are needed for $\overline{w'w'c'}$ and $\overline{\theta'c'}$ and a parameterization for the pressure term is required to close the system of equations. An approximate expression for $\overline{w'w'c'}$ is obtained by examination of its budget equation:

$$\langle\overline{w'^2c'}\rangle = \frac{\tau}{C_1}\left[-\langle\overline{w'^3}\rangle\frac{\partial\langle\bar{c}\rangle}{\partial z} - \langle\overline{w'c'}\rangle\frac{\partial\langle\overline{w'^2}\rangle}{\partial z}\right.$$

$$\left. - 2\langle\overline{w'^2}\rangle\frac{\partial\langle\overline{w'c'}\rangle}{\partial z}\right], \tag{13a}$$

$$\tau = q^2/\varepsilon, \tag{13b}$$

where τ is a turbulence time scale, and ε is the dissipation rate of the turbulent kinetic energy (TKE), defined as $\mathrm{TKE} = q^2/2$, where $\overline{q^2} = \overline{u'^2} + \overline{v'^2} + \overline{w'^2}$. These are computed quantities from a canopy turbulence flow field model presented by Meyers and Paw U (1986).

The conservation equation for the buoyancy term $\langle \overline{\theta' c'} \rangle$ is

$$\frac{\partial \langle \overline{\theta' c'} \rangle}{\partial t} = 0 = -\langle \overline{w' c'} \rangle \frac{\partial \langle \bar{\theta} \rangle}{\partial z} - \langle \overline{w' \theta'} \rangle \frac{\partial \langle \bar{c} \rangle}{\partial z} - \frac{\partial \langle \overline{w' \theta' c'} \rangle}{\partial z} - 2\langle \varepsilon \rangle_{\theta c} \tag{14}$$

T2 D2

where the transport term (T2) and molecular dissipation rate (D2) of the scalar covariance are expressed as

$$\langle \overline{w' \theta' c'} \rangle = \frac{\tau}{C_1} \left[-\langle \overline{w'^2 c'} \rangle \frac{\partial \langle \bar{\theta} \rangle}{\partial z} - \langle \overline{w'^2 \theta'} \rangle \frac{\partial \langle \bar{c} \rangle}{\partial z} - \langle \overline{w'^2} \rangle \frac{\partial \langle \overline{\theta' c'} \rangle}{\partial z} - \langle \overline{w' \theta'} \rangle \frac{\partial \langle \overline{w' c'} \rangle}{\partial z} - \langle \overline{w' c'} \rangle \frac{\partial \langle \overline{w' \theta'} \rangle}{\partial z} \right], \tag{15a}$$

$$\langle \varepsilon \rangle_{\theta c} = C_2 \frac{\langle \overline{\theta' c'} \rangle}{\tau}. \tag{15b}$$

The pressure term in eq. (12) was modeled as

$$\left\langle \frac{\overline{c' \partial p'}}{\partial z} \right\rangle = C_3 \frac{\langle \overline{w' c'} \rangle}{\tau} - \tfrac{1}{3} g \beta \langle \overline{\theta' c'} \rangle. \tag{16}$$

The constants C_2 and C_3 were determined by assuming local equilibrium between gradient production and pressure (or molecular) destruction of $\overline{\theta' c'}$ for an adiabatic wind field.

The equations were solved numerically on a vertical grid of 60 equally spaced points spanning 3 canopy heights. The numerical procedures for determining the turbulent flow field, energy fluxes, concentration profiles and pollutant fluxes are discussed in Meyers and Paw U (1986, 1987) and Meyers (1987), respectively.

Input data needed to run the model include measurements of $(\bar{u})$, air temperature, humidity, pollutant concentration, and global radiation at some point above the canopy. Structural information includes vertical profiles of leaf area, an effective leaf drag coefficient (C_d), and the canopy height (H_c).

4. Chemical flux measurements

Measurements of SO_2 and O_3 fluxes were made over an east Tennessee oak-hickory forest (described in Hutchinson et al., 1986) with the eddy correlation technique. The fluxes were measured at 30 m, 7 m above the mean canopy height. A three-dimensional sonic anemometer (Applied Technology, Boulder, CO) measured the wind velocity components. Measurements of O_3, SO_2, air temperature and absolute humidity were sampled at 10 Hz with fast response instrumentation; the instruments are described in Matt et al. (1988). Fluxes were computed as the mean covariance between the vertical velocity fluctuation and the fluctuation in the entity of interest, averaged over 30 min. A 200 s running mean was used to detrend the time series and to determine the instantaneous fluctuations. A three-dimensional coordinate rotation was performed on the 30 min averaged data to correct for instrument misalignment and for the influence of complex terrain on the mean streamlines. Corrections for density fluctuations due to heat and moisture exchange were made using the technique described by Webb et al. (1980). Flux data were not used when mean concentrations were less than 1 ppb because of the uncertainty in the concentration measurements.

Ancillary measurements included global radiation, net radiation, and soil moisture. Stomatal resistance measurements were taken periodically to monitor the water stress of the trees surrounding the tower where the fluxes were measured.

Two separate studies were conducted. One study was made in August, 1986, during a period when the forest had been exposed to a prolonged period of drought. Another study was conducted in July of 1985 when only measurements of SO_2 flux were made (see Matt et al. (1987)). These data are from a period when the canopy was generally well-watered.

5. Computational procedure

The parameters on which the model computations are based are presented in Table 1. Models I and II assume that: (a) all leaves within the canopy are exposed to the same concentration levels; (b) leaf temperature is equal to the air temperature measured above the canopy (also for model III). For the multi-layer models, continuous vertical profiles of leaf area density were derived by fitting empirical data with the

Beta distribution (Massman, 1982; Meyers, 1987).

6. Results

6.1. *Model predictions of deposition to a deciduous forest*

Model predictions and flux measurements for the July 1985 case study (see Matt et al., 1988) are shown in Fig. 2; chemical and meteorological data are presented in Table 2. The more detailed multi-layer models provide better estimates of the SO_2 flux rates for the well-watered forest than do the simpler single layer of "big leaf" models (i.e., models I and II). The root mean square errors (rmse) of the multi-layer models are generally one-half of those from the single layer models (Table 3).

The pattern in the relative errors between the models for the water-stressed forest in the August 1986 study is nearly identical to the July, 1985,

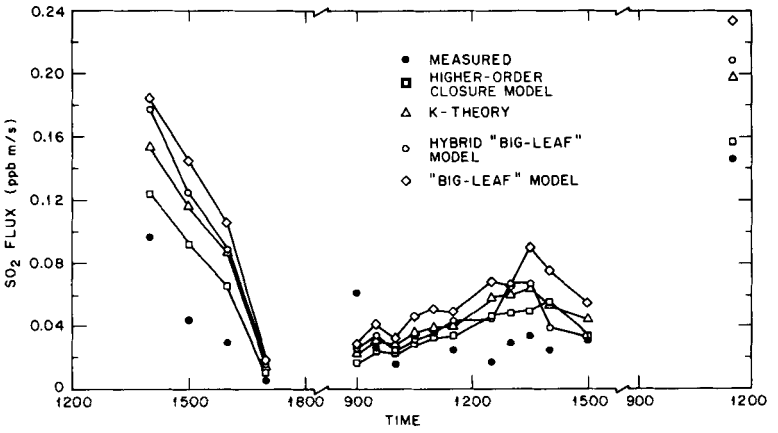

Fig. 2. Time series of measured and modeled SO_2 fluxes to a well-watered forest (July, 1985, experiment).

Table 2. *Meterological and chemical data from July 1985 experiment*

Julian day	Time (EST)	$[SO_2]$ (ppbv)	(V_d) (cm s^{-1})	$(\bar{u})$ (m s^{-1})	$\bar{\theta}$ (°C)	RH (%)	R_g (W m^{-2})
189	1400	14.6	(0.66)	2.6	27.9	62	629
189	1500	10.8	(0.41)	3.4	28.0	61	637
189	1600	8.8	(0.35)	3.1	28.6	57	508
189	1700	1.6	(0.33)	3.0	29.1	55	497
190	0930	3.3	(0.83)	2.6	24.9	72	456
190	1000	3.0	(0.54)	3.0	25.3	72	460
190	1030	3.5	(0.87)	2.5	26.6	71	756
190	1100	3.8	(1.00)	2.1	26.9	72	705
190	1130	3.9	(0.64)	2.3	27.2	70	701
190	1230	5.7	(0.31)	2.2	28.4	68	626
190	1300	6.4	(0.46)	1.7	28.4	66	528
190	1330	6.6	(0.52)	1.5	28.9	66	771
190	1400	6.0	(0.42)	1.2	29.2	65	855
190	1500	5.0	(0.62)	2.5	29.2	65	356
191	1130	17.8	(0.82)	4.0	27.8	69	628

The mean wind $(\bar{u})$, SO_2 concentration corresponding deposition velocity (V_d), air temperature $(\bar{\theta})$, global radiation (R_g), and relative humidity (RH) were measured at 30 m.

experiment for both SO_2 and O_3 (Table 3). However, all four models significantly over-estimate the observed SO_2 and O_3 flux rates when water stress is not accounted for (Figs. 3, 4, open triangles) giving relatively larger rmse values (chemical and meteorological data for the August 1986 study are presented in Table 4).

Table 3. *Root mean square errors (rmse) between modeled and predicted sulfur and ozone fluxes over deciduous forest*

	Model I	Model II	Model III	Model IV
	(units = ppb m s^{-1})			
July 1985				
(SO_2)	0.052	0.040	0.026	0.023
August 1986				
water stress not considered				
(SO_2)	0.026	0.022	0.013	0.013
(O_3)	0.490	0.425	0.197	0.214
water stress considered				
(SO_2)	0.010	0.009	0.014	0.010
(O_3)	0.242	0.226	0.075	0.086

The "no stress $r_{s,min}$" refers to using the tabulated minimum stomatal resistance while the "stress $r_{s,min}$" uses measured values of the minimum stomatal resistance.

During some of the experimental periods in August, 1986, simultaneous measurements of stomatal resistance were made on oak leaves close to the tower. These data reveal that the canopy was experiencing moderate to severe water stress (Fig. 5). Consequently, consideration of only PAR and leaf temperature in the stomatal resistance submodel did not fully account for the relatively large resistances observed. The diurnal increase in vapor pressure deficits probably did not cause stomatal closure in the afternoon because an analysis of the stomatal resistance data for oak revealed no dependency on vapor pressure deficits (Fig. 6). Similar results have been reported by Appleby and Davies (1983). Chemical saturation in the leaf mesophyll and leaf water potential are probable causes for the higher measured resistances and corresponding lower observed fluxes. Obviously, the effects of low leaf water potentials must be considered during water stress conditions. We were not able to measure leaf water potential directly and its effect on stomatal resistance because the appropriate instrumentation was not available. However, we were able to estimate the factor $f(\omega)$ as the ratio of direct measurements of stomatal resistance to r_s computed from eq. (4) for well-

Table 4. *Meterological and chemical data from August 1986 experiment*

Julian day	Time (EST)	[SO_2] (ppbv)	(V_d) (cm s^{-1})	[O_3] (ppbv)	(V_d) (cm s^{-1})	($\bar{u}$) (m s^{-1})	$\bar{\theta}$ (°C)	RH (%)	R_g (W m^{-2})	$f(\omega)$
234	1230	4.1	(1.14)	51.7	(0.37)	1.4	27.0	74	519	0.40
234	1300	4.3	(0.87)	51.8	(0.48)	1.7	27.2	72	431	0.45
234	1330	4.4	(0.56)	57.3	(0.42)	1.5	28.2	67	737	0.50
234	1400	4.2	(0.39)	59.3	(0.43)	1.5	28.8	65	866	0.50
234	1430	4.0	(0.58)	62.5	(0.30)	2.1	28.8	62	747	0.50
234	1600	2.8	(0.54)	60.4	(0.43)	2.0	28.9	61	577	0.50
234	1630	3.2	(0.89)	62.7	(0.38)	1.8	29.1	61	467	0.50
234	1700	3.7	(0.39)	63.0	(0.19)	2.1	29.1	61	353	0.50
234	1730	3.5	(0.26)	60.2	(0.27)	2.2	28.9	61	257	0.50
235	0930	3.8	(0.21)	24.6	(0.83)	2.0	24.3	84	525	—
235	1000	4.4	(0.42)	31.1	(0.47)	1.8	25.1	81	621	—
235	1030	4.1	(0.28)	34.9	(0.69)	2.0	25.8	77	697	0.50
235	1330	2.4	(1.13)	35.6	(0.31)	2.6	27.7	71	457	0.50
235	1400	1.9	(0.86)	32.2	(0.26)	2.6	28.0	70	402	0.50
235	1500	1.2	(0)	32.2	(0.30)	2.8	29.0	64	571	0.50
235	1530	1.4	(0)	33.0	(0.42)	2.6	28.9	63	280	0.50

The mean wind ($\bar{u}$), relative humidity (RH) and global radiation (R_g) were measured at 30 m. The SO_2 and O_3 concentrations and corresponding deposition velocities (V_d) were measured on a tower some 250 m to the northeast. The last column is the estimated correction factor for stomatal resistance due to leaf water potential.

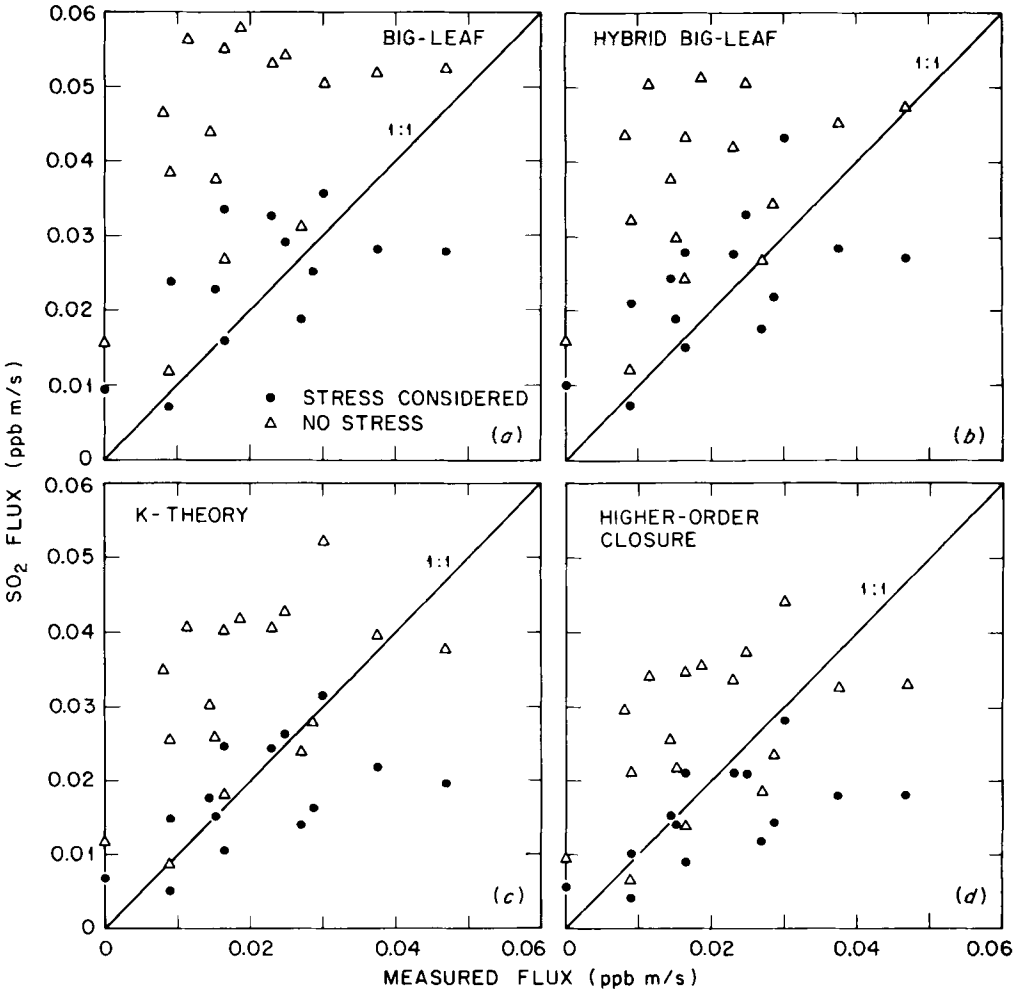

Fig. 3. Measured and modeled SO_2 fluxes to a water stressed forest (August, 1986, experiment). Closed circles (●) include water stress correction in models while open triangles (△) represent no correction for water stress.

watered conditions, including the dependency on PAR and leaf temperature. This factor was then incorporated into the models, whereby the model computations were repeated (Figs. 3 and 4, closed circles). For SO_2, the root mean square error (rmse) values from models I and II were about one-half the values from the original flux estimates while those from model III and IV were moderately improved. For O_3, incorporating the modified stomatal resistance reduced the rmse by a factor of two for all models. The use of this inferred $f(\omega)$ factor reduces the rmse for models III and IV by a greater percentage for O_3 than for SO_2. We believe the greater improvement in the estimate of O_3 fluxes relative to those of SO_2 can be attributed to more reliable measurements in the O_3 concentrations and fluxes because of the greater O_3 concentration levels and less "noisy" instrumentation (see Wesely and Hart (1985)).

6.2. Discussion

Scrutiny of the comparison of measured and calculated fluxes reveals that none of the models tested simulate dry deposition in the afternoon as well as during the morning hours. From the available measurements, we could account for the

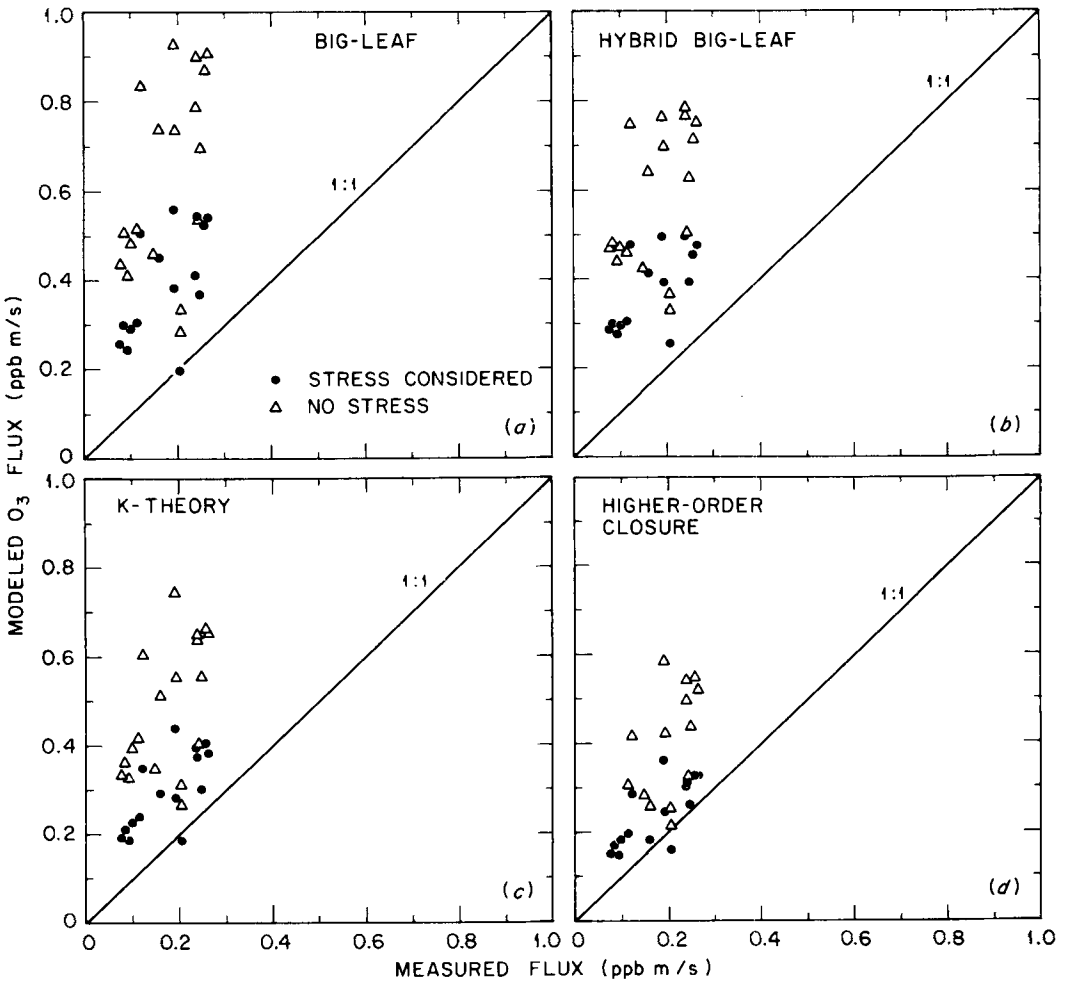

Fig. 4. Measured and modeled O_3 fluxes to a water stressed forest (August, 1986, experiment). Closed circles (●) include water stress correction in models while open triangles (△) represent no correction for water stress.

lower fluxes observed in the afternoon as indicated by the high stomatal resistances. However, we could not pinpoint the cause of the high resistances but speculate that temporary afternoon water deficits, effects of chemical saturation in the leaf mesophyll, or other chemical resistances due to reactions in the stomatal cavity probably were occurring, perhaps simultaneously.

Multi-layer models integrate the non-linear detailed processes that occur on a leaf scale to derive the net uptake for the entire canopy. The net chemical uptake on a leaf scale is governed by the chemical concentration just outside the leaf boundary layer, the stomatal resistance (r_s) which is a function of light and other factors (see eq. 4), and the leaf boundary layer resistance (r_b), which is non-linearly dependent on the local wind speed. The increasing complexity in going from model I to IV gives improved estimates of the measured fluxes since the local environments where the transfer is actually occurring are modeled more accurately.

For example, the improvement of model II over model I is the result of an improved representation of the canopy resistance (R_c) by including a radiative transfer model to estimate the

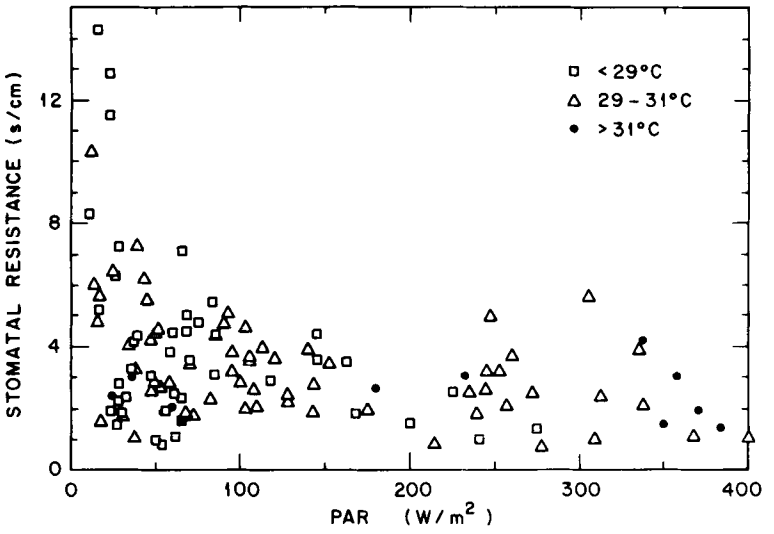

Fig. 5. Stomatal resistance dependency on incident photosynthetically active radiation (PAR).

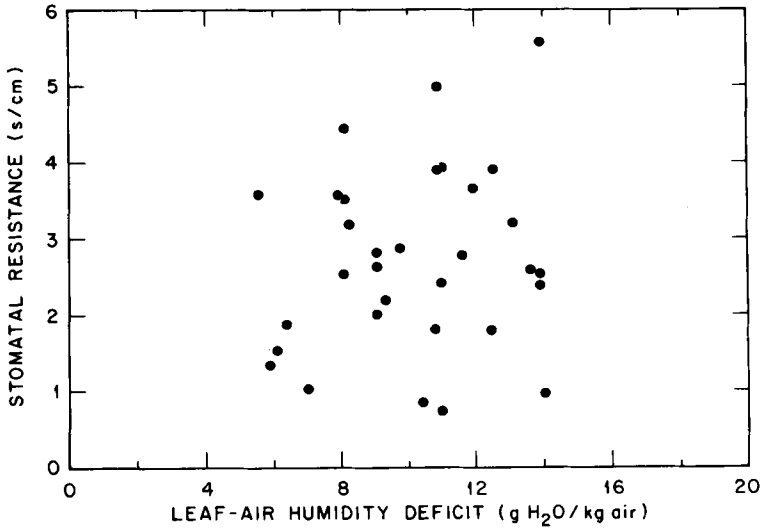

Fig. 6. Dependence of stomatal resistance on leaf-air humidity deficit.

PAR regime throughout the canopy for sunlit and shaded leaves. This results in generally a 15% reduction in rmse values. Such a treatment is crucial because the sink strength for SO_2 and O_3 is dominated by stomatal uptake.

The improved estimate of model III over model II is due to a more detailed treatment of both turbulent diffusion within the canopy and molecular diffusion through the viscous sublayer on the leaf surfaces. A 30% reduction in the rmse, under well-watered conditions, is seen in using model III over model I.

Model IV improves upon model III's treatment of within-canopy diffusion by incorporating

higher-order-closure concepts, thereby eliminating the need to relate vertical turbulent fluxes directly to concentration gradients using a within-canopy turbulent diffusion coefficient. The other major improvement of model IV over model III is the incorporation of leaf energy balance equations which provide estimates of leaf temperatures for shaded leaves and nine leaf angle classes of sunlit leaves to be used in eq. (4). These improvements result in rmse values that are generally 45% lower than model I.

Model III is a "*K*-theory" turbulent diffusion model for transport of passive contaminants. "*K*-theory" concepts have been criticized for applications to plant canopies (see Legg and Monteith (1975), Finnigan and Raupach (1987)), since these models are valid for describing vertical diffusion only when the vertical length scale of the turbulent transfer is smaller than the length scale associated with the change in the vertical concentration gradient (Corrsin, 1974). This constraint is often not met within the plant canopies because turbulence is an intermittent process, driven by large eddies. In addition, "*K*-theory" cannot reproduce the counter-gradient transport structure that is frequently observed in plant canopies (Denmead and Bradley, 1985). The criticism of "*K*-theory" models is especially valid for water vapor, sensible heat and CO_2 exchange since these entities are associated with gradients that change on smaller scales than those associated with the turbulence. Under situations with low leaf resistances to pollutant (r_ℓ) uptake, the computation of the concentration gradient inside the canopy is crucial in making accurate computations of pollutant uptake. Bache (1986) theoretically computed that the error in the deposition velocity, when assuming a constant concentration profile is about 50% when r_ℓ is on the order of 100 s/m. On the other hand, this error is less than 15% when r_ℓ exceeds 500 s/m.

A comparison of SO_2 modeled concentration and uptake profiles from model III and IV for three different above-canopy wind velocities is shown in Figs. 7 and 8, respectively. In Fig. 8, the SO_2 uptake intensity, which is defined as the mass of SO_2 diffusing into leaves per unit volume each second, is equivalent to the vertical divergence of the chemical flux and is computed from eq. 8. Because the SO_2 sink strength is proportional to the plant area density, some of

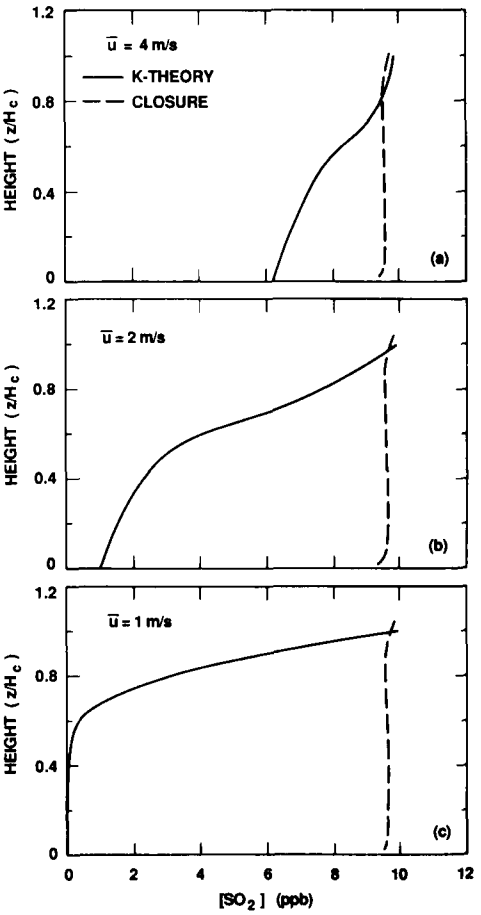

Fig. 7. Mean SO_2 concentration profiles from models III and IV for 3 wind speed values taken at 1.5 canopy heights (Hc).

the differences between models III and IV may be due to the fitted vertical profile of leaf area because model III used 40 layers within the canopy while model IV uses 20 layers. The flux and concentration profiles from model III vary considerably with the above-canopy mean wind velocity, while those from model IV are relatively unchanged. The mean concentration profiles from model III are more sensitive to wind speed because in model III, the fluxes are proportional to the concentration gradients. Since the uptake of SO_2 is mainly limited by stomatal diffusion, the potential for a canopy to take up pollutants will not vary substantially with changes in the

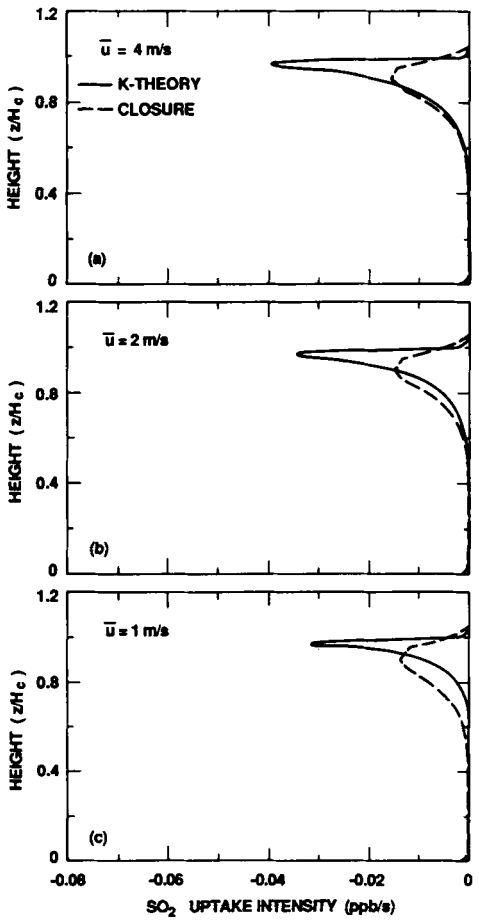

Fig. 8. SO_2 uptake intensity profiles from models III and IV for 3 wind speed values taken at 1.5 canopy heights (Hc).

wind speed. However, in "*K*-theory" models, sustaining the flux in low wind conditions requires that gradients in the mean concentration be large because the eddy diffusivity is smaller. The large modeled gradients for the lower wind speed regime narrows the SO_2 uptake profile (Fig. 8) because the uptake intensities are proportional to the mean concentration at any particular layer. For model IV, the modeled mean concentration SO_2 uptake intensity profiles change only slightly with wind speed. For low wind speed and identical global radiation values for the higher wind case, more energy is partitioned into sensible heat; hence more vertical mixing occurs due to buoyancy which tends to decrease the gradients. For the higher wind speed cases, there is enhanced vertical mixing from mechanically driven turbulence which also tends to decrease the concentration gradients. This is reflected in the narrower range of modeled deposition velocities for model IV versus model III.

Overall, the deposition velocities for models III and IV agree rather well (Table 5). For moderate to high wind speeds, the simulated concentration gradients from models III and IV are in general agreement in the upper 80% of the canopy where over 75% of the foliage is distributed. Although model III's simulated gradients show more sensitivity to wind speed because the fluxes are proportional to the concentration gradients, the errors in modeled concentration deep within the canopy are not serious for foliar deposition estimates because of the lack of foliage there. Thus, the limitations associated with "*K*-theory" may not be as crucial for canopies of similar structure. However, additional model comparisons on more uniform plant area distributions are needed to assess the overall uncertainties.

Obviously, there are trade-offs among the physical and biological representativeness in detailed models vs simple models and the computational run-time, ease of use, and number of parameters needed to implement the models. For identifying and evaluating the important processes that occur on leaf scales and performing sensitivity analyses, the more detailed models are appropriate. From a routine monitoring standpoint, models such as I and II are more appropriate because of their computational efficiency and the limited number of meteorological and

Table 5. *Deposition velocities (V_d) from "K-theory" and higher-order closures models for various wind regimes*

	$\bar{u}$ at 1.5 Hc		
	1 m s^{-1}	2 m s^{-1}	4 m s^{-1}
	V_d (cm s^{-1})		
K-theory	0.67	0.96	1.11
higher-order closure	0.76	0.82	0.86

biological measurements that are required. However, with any of these models, users should proceed with clear awareness of the model assumptions and associated uncertainties and limitations.

7. Conclusions and recommendations

A hierachy of models for computing dry deposition fluxes of SO_2 and O_3 has been presented. We found that increasing the complexity of the submodels that parameterize the physical exchange processes improved the estimates of the deposition rates. For SO_2 and O_3, the deposition rate is limited by the stomatal resistance. By incorporating measured values of the stomatal resistance into the models, rmse values were reduced by generally 50% under water stressed conditions.

Most, if not all, gaseous deposition models are subject to uncertainty in the values of $r_{s,min}$ and the corresponding correction factors. Periodic measurements of stomatal resistance, soil moisture, and a "site-calibrated" determination of the minimum stomatal resistance under well-watered conditions for the species under study can only improve the predictability of any model because $r_{s,min}$ values generally must otherwise be taken from the literature. Such tabulated values generally have large uncertainties for any particular species or classification of plants (see Korner et al. (1979)).

8. Acknowledgements

We would like to thank R. P. Hosker and W. R. Pendergrass for their helpful comments and suggestions on this paper. We especially acknowledge D. R. Matt and J. D. Womack for maintaining and operating the chemical sensors during the field experiments. This work was conducted as a contribution to the National Acid Precipitation Assessment Program (Task Group II, Atmospheric Chemistry) under the sponsorship of the National Oceanic and Atmospheric Administration and the US Department of Energy.

REFERENCES

Appleby, R. F. and Davies, W. J. 1983. A possible evaporation site in the guard cell wall and the influence of leaf structure on the humidity response by stomata of woody plants. *Oecologia 56*, 30–40.

Bache, D. H. 1986. On the theory of gaseous transport to plant canopies. *Atmos. Environ. 20*, 1379–1388.

Baldocchi, D. D. 1988. A multi-layer model for estimating sulphur dioxide deposition to a deciduous oak forest canopy. *Atmos. Environ.*, in press.

Baldocchi, D. D., Hicks, B. B. and Camara, P. 1987. A canopy stomatal resistance model for gaseous deposition to vegetated canopies. *Atmos. Environ. 21*, 91–101.

Baldocchi, D. D., Hutchison, B. A., Matt, D. R. and McMillen, R. T. 1985. Canopy radiative transfer models for spherical and known leaf inclination angle distributions: a test in an oak-hickory forest. *J. Applied Ecology 22*, 539–555.

Corrsin, S. 1974. Limitations on gradient transport models in random walks and in turbulence. *Adv. Geophys. 18A*, 25–60.

Denmead, O. T. and Bradley, E. F. 1985. Flux-gradient relationships in a forest canopy. In *Forest-atmosphere interactions* (eds. B. A. Hutchison and B. B. Hicks). Dordrecht/Holland: Reidel Publ. Comp., 421–442.

Eckert, E. R. G. and Gross, J. F. 1963. *Introduction to heat and mass transfer*. New York: McGraw-Hill, 346 pp.

Finnigan, J. J. 1985. Turbulent transport in flexible plant canopies. In *Forest-atmosphere interactions* (eds. B. A. Hutchison and B. B. Hicks). Dordrecht/Holland: Reidel Publ. Comp., 443–480.

Finnigan, J. J. and Raupach, M. R. 1987. Modern theory of transfer in plant canopies in relation to stomatal characteristics. In *Stomatal function* (eds. E. Zeiger, G. Farquhar and I. Cowan). Stanford, CA: Stanford University Press, 385–429.

Grace, J. and Wilson, J. 1976. The boundary layer over a Populus leaf. *J. Experimental Botany 27*, 231–241.

Hicks, B. B., Baldocchi, D. D., Meyers, T. P., Hosker, R. P. and Matt, D. R. 1987. A preliminary multiple resistance routine for deriving dry deposition velocities from measured quantities. *Water, Air and Soil Pollution 36*, 311—330.

Hosker, R. P. 1986. Practical application of air pollutant deposition models—current status, data requirements and research needs. *Proc. Internat. Conf. on Air Pollutants and their Effects on the Terrestrial Ecosystem* (eds. A. M. Legge and S. V. Krupa), New York: Wiley and Sons, 546–567.

Hutchinson, B. A., Matt, D. R., McMillen, R. T., Gross, L. J., Tajchman, S. J. and Norman, J. M. 1986. The architecture of an east Tennessee deciduous forest canopy. *J. Ecol. 74*, 635–646.

Jarvis, P. G. 1976. The interpretation of the variations in leaf water potential and stomatal conductance

found in canopies in the field. *Phil. Trans. R. Soc. Lond. B 273*, 593–610.

Korner, C., Scheel, J. A. and Bauer, H. H. 1979. Maximum leaf diffusive conductance in vascular plants. *Photosynthetica 13*, 45–82.

Legg, B. J. and Monteith, J. 1975. Heat and mass transfer in plant canopies. In *Heat and mass transfer in the biosphere* (eds. D. A. DeVries and H. H. Afgan). New York: Wiley and Sons, 167–186.

Mansfield, T. A. 1985. Porosity at a price: the control of stomatal conductance in relation to photosynthesis. In *Photosynthetic mechanisms and the environment* (eds. J. Barber and N. R. Baker). Elsevier Science Publishers, 419–452.

Massman, W. J. 1982. Foliage distribution in old-growth coniferous tree canopies. *Can. J. For. Res. 12*, 10–17.

Matt, D. R., McMillen, R. T., Womack, J. D. and Hicks, B. B. 1987. A benchmark comparison of estimated and measured SO_2 deposition velocities. *Water, Air and Soil Pollution 36*, 331–347.

Meyers, T. P. 1987. The sensitivity of modeled fluxes and profiles to leaf stomatal and boundary layer resistances. *Water, Air and Soil Pollution 35*, 261–278.

Meyers, T. P. and Paw U, K. T. 1986. Testing of a higher-order closure model for airflow within and above plant canopies. *Boundary-Layer Meteorol. 37*, 297–311.

Meyers, T. P. and Paw U, K. T. 1987. Modeling the plant canopy microenvironment with higher-order closure principles. *Agric. Forest Meteorol. 41*, 143–163.

Monteith, J. L. 1973. *Principles of environmental physics*. London: E. Arnold, 241 pp.

Murphy, C. E., Jr., Sinclair, T. R. and Knoerr, K. R. 1977. An assessment of the use of forests as sinks for the removal of atmospheric sulfur dioxide. *J. Environmental Quality 6*, 388–396.

Norman, J. M. 1979. Modeling the complete crop canopy. In *Modification of the aerial environment of crops* (eds. B. J. Barfield and J. F. Gerber). ASAE Monograph 2, Michigan: St. Joseph, 249–277.

Raupach, M. R., Coppin, P. A. and Legg, B. J. 1986. Experiments on scalar dispersion within a model plant canopy. Part I: the turbulent structure. *Boundary-Layer Meteorol. 35*, 21–52.

Ross, J. 1976. Radiative transfer in plant communities. In *Vegetation and the atmosphere 1* (ed. J. L. Monteith). London: Academic Press, 13–55.

Schuepp, P. H. 1977. Tubulent transfer at the ground: on verification of a simple predictive model. *Boundary-Layer Meteorol. 12*, 171–186.

Shreffler, J. H. 1976. A model for the transfer of gaseous pollutants to a vegetational surface. *J. Applied Meteorology 15*, 744–746.

Thom, A. S. 1975. Momentum, mass and heat exchange of plant communities. In *Vegetation and the atmosphere 1* (ed. J. L. Monteith). London: Academic Press, 57–109.

Verma, S. B., Baldocchi, D. D., Anderson, D. E., Matt, D. R. and Clement, R. J. 1986. Eddy fluxes of CO_2, water vapor and sensible heat over a deciduous forest. *Bound. Layer Meteorol. 36*, 71–91.

Waggoner, P. E. 1975. Micrometeorological models. In *Vegetation and the atmosphere 1* (ed. J. L. Monteith). London: Academic Press, 205–228.

Webb, P. E., Pearman, G. I. and Leuning, R. 1980. Correction of flux measurements for density effects due to heat and water vapor transfer. *Quart. J. R. Met. Soc. 106*, 85–100.

Weiss, A. and Norman, J. M. 1985. Partitioning solar radiation into direct and diffuse, visible and near-infrared components. *Agric. Forest Meteorol. 34*, 205–213.

Wesely, M. L. and Hart, R. L. 1985. Variability of short term eddy-correlation estimates of mass exchange. In *The forest-atmosphere interaction* (eds. B. A. Hutchison and B. B. Hicks). Dordrecht/Holland: D. Reidel Publ. Comp., 591–612.

Wesely, M. and B. B. Hicks. 1977. Some factors that affect the deposition rates of sulfur dioxide and similar gases on vegetation. *J. Air. Poll. Cont. Assoc. 27*, 1110–1116.